

1 **Genome-wide association study of DXA-derived hip**  
2 **morphology identifies associations with 4 loci in Chinese**  
3 **populations**

4 Jiayi Zheng<sup>1</sup>, Jieyu Ge<sup>1</sup>, Benjamin G. Faber<sup>2,3</sup>, Huandong Lin<sup>4,5</sup>, Raja Ebsim<sup>6</sup>,  
5 Claudia Lindner<sup>6</sup>, Timothy Cootes<sup>6</sup>, Jin Li<sup>7</sup>, Jonathan H. Tobias<sup>2,3</sup>, Xin Gao<sup>4,5</sup>,  
6 Sijia Wang<sup>1</sup>

7

8 **Affiliations:**

- 9 1) CAS Key Laboratory of Computational Biology, Shanghai Institute of  
10 Nutrition and Health, University of Chinese Academy of Sciences, Chinese  
11 Academy of Sciences, Shanghai, China.  
12 2) Musculoskeletal Research Unit, University of Bristol, UK  
13 3) Medical Research Council Integrative Epidemiology Unit at the University  
14 of Bristol, UK  
15 4) Department of Endocrinology and Metabolism, Zhongshan Hospital,  
16 Fudan University, Shanghai, China.  
17 5) Fudan Institute for Metabolic Diseases, Shanghai, China  
18 6) Division of Informatics, Imaging and Data Sciences, The University of  
19 Manchester, UK  
20 7) Human Phenome Institute, Fudan University, Shanghai, China  
21

## 22 Abstract

### 23 Objective:

24 To identify genetic factors associated with hip morphology in Chinese  
25 populations.

26

### 27 Methods:

28 An 85-point Statistical Shape Model (SSM) was applied to extract hip shape  
29 modes (HSMs). Diameter of the femoral head (DFH), femoral neck width  
30 (FNW) and hip axis length (HAL) were obtained from SSM points using Python  
31 scripts. Genome-wide association study (GWAS) was conducted in the  
32 Shanghai Changfeng (SC) cohort (N=5,310) for each phenotype of  
33 DXA-derived hip morphology. Replication of GWAS was conducted in the Core  
34 cohort (N=917).

35

36 Results: GWAS identified a total of 331 SNPs in 14 loci that were associated  
37 with features of hip morphology in the SC cohort. 4 of 14 loci were replicated in  
38 the Core cohort: rs143383 (*GDF5*) associated with HAL ( $P = 9.4 \times 10^{-10}$ ),  
39 rs11614913 (*MIR196A2*) associated with HSM9 ( $P = 2.8 \times 10^{-10}$ ), rs35049516  
40 (*SUPT3H*) associated with HSM4 ( $P = 4.3 \times 10^{-10}$ ) and rs7761119 (*UST*)  
41 associated with HSM8 ( $P = 1.7 \times 10^{-8}$ ). Of these, two loci were known to affect  
42 hip morphology, including rs143383 (*GDF5*) and rs35049516 (*SUPT3H*),  
43 whereas rs11614913 (*MIR196A2*) and rs7761119 (*UST*) were novel. There  
44 was also overlap with previous GWAS of HSM and other hip-based metrics.

45

### 46 Conclusions:

47 In the largest East Asian ancestry hip shape GWAS to date we identified and  
48 replicated four loci associated with different aspects of hip morphology (*GDF5*,  
49 *MIR196A2*, *SUPT3H*, *UST*). Strong SNP-to-gene evidence was found. All four  
50 loci have previously been implicated in musculoskeletal development, however  
51 this is the first report that rs11614913 (*MIR196A2*) and rs7761119 (*UST*) are  
52 associated with hip morphology. Despite the small sample size, this study  
53 paves the way for trans-ancestry meta-analyses.

## 54 Keywords

55 hip morphology, genome-wide association study, Chinese

56

## 57 **Introduction**

58 Hip morphology is considered to be an important risk factor for hip  
59 osteoarthritis (HOA) (1). Our recent study found a much lower prevalence of  
60 radiographic HOA (rHOA) in the Shanghai Changfeng (SC) cohort, a  
61 community-based Chinese study, when compared to white participants in UK  
62 Biobank (UKB), a community-based UK study (2). These results were  
63 consistent with previous studies in other East Asian populations (3, 4, 5). In  
64 addition, distinct differences in hip morphology were seen between SC and  
65 UKB participants. For example, there was a lower prevalence of cam  
66 morphology, a narrower femoral neck, and a larger femoral head relative to  
67 femoral neck in the East Asian participants (SC) compared with the white  
68 participants (UKB). It is unclear if these differences in hip morphology and  
69 rHOA between SC and UKB are related, and to what extent these result from  
70 genetic as opposed to environmental differences.

71  
72 Hip morphology derived from imaging can be characterized by statistical  
73 shape modelling (SSM), a form of principal component analysis, which  
74 computes orthogonal hip shape modes (HSMs) (6, 7). Whereas SSM  
75 describes the overall shape, geometric parameters measure specific hip  
76 morphology, for example, femoral neck width (FNW) or hip axis length (HAL).  
77 Previously, SSM-derived hip morphology formed the basis of a genome wide  
78 association study (GWAS) (8), which identified eight loci associated with  
79 pathways involved in endochondral bone formation. In addition, GWAS has  
80 examined geometric parameters of hip shape such as alpha angle (a measure  
81 of cam morphology) and minimum joint space width, providing valuable  
82 insights into osteoarthritis pathogenesis (9, 10). These studies were based in  
83 European populations, limiting the conclusions that could be applied to other  
84 ancestry groups.

85  
86 Using previously derived measures of hip shape in SC, this study aims to  
87 provide the first comprehensive GWAS of hip shape in an East Asian  
88 population, including both HSMs and hip geometric parameters, namely FNW,  
89 HAL and diameter of the femoral head (DFH). Subsequently, we aimed to  
90 understand the extent to which hip shape associated loci overlap with other  
91 hip-based metrics including hip bone size, HOA, hip fracture and femoral neck  
92 bone mineral density (FN BMD).

93

## 94 **Materials and methods**

### 95 **Participants in discovery set**

96 SC consists of residents recruited from the Changfeng community of the Putuo

97 District in Shanghai (N=6595, aged  $\geq 45$  years) between June 2009 and  
98 December 2012 (11). The Shanghai Changfeng Study is organized and  
99 directed by The Fudan-Erasmus Research Institute of Medicine (FERIM),  
100 which is a joint venture between Zhong Shan Hospital of Fudan University in  
101 Shanghai and the Erasmus Medical Center, Rotterdam, The Netherlands.  
102 Ethics approval was granted by the ethics committee of Zhongshan Hospital  
103 affiliated to Fudan University (B2008-119(3)) and written informed consent was  
104 provided by all participants before participation. All participants answered a  
105 survey and the majority had a high-resolution iDXA (GE Lunar) scans of their  
106 left hip (N=6082). Quality control identified 144 images of low-quality, 6  
107 repetitious scans, and 622 samples without genomic data. The remaining 5310  
108 samples were included in the GWAS analysis.

109

### 110 **Participants in replication**

111 Participants in the Core cohort have been recruited by Fudan University in  
112 Shanghai since September 2018. The samples we included in this study were  
113 recruited before August 2022 (N=916, aged 20 to 60 years). High-resolution  
114 iDXA (GE Lunar) scans of their left hip were taken. All samples included in this  
115 study passed quality control of low-quality left hip DXA scans or low-quality  
116 gene data. Written informed consent was provided before participation. The  
117 Core cohort was recruited by Human Phenome Data Center of Fudan  
118 University and is still in expansion.

119

### 120 **Phenotyping**

#### 121 **Statistical hip shape model**

122 The left hip was outlined in DXAs using 85 points placed by a  
123 machine-learning trained software (BoneFinder®, The University of  
124 Manchester), excluding osteophytes. The point annotations were reviewed  
125 and corrected where necessary. Hip shape size and rotation were  
126 standardized by Procrustes analysis after point placement. Principal  
127 components analysis was then used to build a statistical shape model (SSM)  
128 from all available images in UKB, producing a set of orthogonal modes of  
129 variation. Further analysis focused on the first ten hip shape modes (HSMs),  
130 which explain 86.3% of hip shape variance. Applying the SSM built in UKB and  
131 the existing shape modes, all available images in the SC cohort and Core  
132 cohort were analysed to get comparable mode scores. A more detailed  
133 description of the methods, including positions of the 85 points outlining the hip,  
134 is provided in our previous publication(12).

135

#### 136 **Hip geometric parameters**

137 Custom Python 3.0 scripts were developed and used to automatically derive  
138 FNW, HAL and DFH, as previously described (13, 14). In brief, FNW was  
139 defined as the shortest distance measured between the superior and inferior  
140 side of the femoral neck, with a line-segment approach used to automatically

141 calculate the narrowest distance between the relevant points. DFH was  
142 defined as the distance across the spherical aspect of the femoral head. To  
143 estimate this, a circle of best fit was placed around the femoral head, with the  
144 diameter of the circle taken to represent the DFH in mm. HAL was defined as  
145 the distance from the base of the greater trochanter to the medial aspect of the  
146 femoral head, drawn through the centre of the circle of best fit (used to  
147 calculate DFH), in mm. All images with geometric parameter values beyond  $\pm 2$   
148 standard deviations (SDs) from the mean were reviewed manually.

149

### 150 **Genotyping, imputation and quality control**

151 Genotyping, imputation and quality control (QC) were performed for the SC  
152 cohort as previously described (15). Genomic DNA of the participants were  
153 extracted from peripheral blood leukocytes using QIAGEN (Hilden, Germany)  
154 QIAamp DNA Mini Blood Kit and genotyped with Illumina (San Diego, CA, USA)  
155 Infinium BeadChip genotyping array (707,180 markers). QC was carried out  
156 using PLINK v1.90b4 (16) (i.e. minor allele frequency (MAF)  $> 1\%$ , Genotype  
157 missingness  $< 2\%$ , Hardy-Weinberg  $p > 1e-5$ ). Samples that had a sex  
158 discrepancy between genotypic and reported sex, or had genotype hard call  
159 rate  $< 95\%$ , or deviated from the expected inbreeding coefficient ( $-0.2 < F < 0.2$ )  
160 or were duplicated samples were excluded. We performed pre-phasing and  
161 phasing using SHAPEIT v2r790(17) and imputation with IMPUTE2 v2.3.1(18)  
162 with the 1000 Genomes (1000G) phase 3 data as the reference. QC was  
163 carried out again and 8,393,320 variants with call rate  $> 98\%$ , Hardy-Weinberg  
164 equilibrium  $P > 1e-5$ , MAF  $> 1\%$ , and INFO score  $> 0.8$  were included in the final  
165 analysis. All genomic positions were in reference to hg19/build 37.

166

### 167 **Genome-wide association study (GWAS)**

168 Analyses of HSMs were adjusted for age, sex and the first 10 ancestry  
169 principal components in the SC cohort and Core cohort. Height wasn't included  
170 as a covariate in HSM analyses as HSM scores were already size adjusted by  
171 Procrustes analysis. As height is highly correlated with the hip geometric  
172 parameters (19), analyses of hip geometric parameters were adjusted for age,  
173 sex, height and the first 10 ancestry principal components in the SC cohort and  
174 Core cohort. GWAS was performed using mixed linear models in fastGWA (20).  
175 Significant threshold for our GWAS were set at  $5 \times 10^{-8}$ . Manhattan plots and  
176 QQ plots were generated in the R package qqman(21). The genomic inflation  
177 factor ( $\lambda$ ) was calculated to check for p value inflation on QQ plots.  
178 Conditionally independent variants in each GWAS were identified by  
179 GCTA-COJO (22, 23) with default parameters (-cojo-p  $5 \times 10^{-8}$ , -cojo-wind  
180 10,000kb). Physically closest gene of variants were annotated by dbSNP  
181 (<https://www.ncbi.nlm.nih.gov/SNP/>). Regional linkage disequilibrium plots and  
182 association plots were generated by LocusZoom(24).

183

### 184 **SNP heritability and genetic correlation**

185 SNP-based heritability was estimated using GCTA-GREML(22). Genetic  
186 correlations between hip morphology phenotypes and hip bone mineral density  
187 of both femoral neck and total hip were calculated by a bivariate GREML  
188 analysis in GCTA(25). Hip bone mineral density was measured by iDXA (GE  
189 Lunar) in the SC cohort.

190

### 191 **Overlap with GWAS of other traits**

192 **GWAS of hip-based metrics** All lead SNPs found in the SC hip morphology  
193 GWAS were looked up in GWAS of DXA bone area of the hip (26), FN BMD(27)  
194 and hip fracture(28), and also in the largest osteoarthritis (OA) GWAS (29).

195 **GWAS of hip shape modes** Loci associated with HSMs in the previous  
196 European GWAS of HSMs (8) were looked up in our Chinese HSM GWAS.

197

### 198 **Fine mapping**

199 Functional Mapping and Annotation (FUMA)(30) was applied to identify  
200 candidate genes for each lead variant. CADD v1.3 (Combined Annotation  
201 Dependent Depletion) were used to evaluate the functional consequences of  
202 the variants (31). Regulatory elements of non-coding human genome were  
203 identified using RegulomeDB(32). ChromoHMM were used to the prediction of  
204 chromatin state (core 15-state model) in chondrocytes and osteoblasts(33).  
205 Significant expression quantitative trait locus (eQTL) association (GTEx v8  
206 database, false discovery rate <0.05) (34, 35, 36) with the lead variant were  
207 looked up.

208

## 209 **Results**

### 210 **Hip morphology GWAS**

211 In this study, we conducted a GWAS for 13 measures of hip morphology  
212 including 10 HSMs, FNW, HAL and DFH. Our discovery GWAS were  
213 conducted in the SC cohort, comprising 5310 individuals (3047 females and  
214 2263 males) with an average age of 63.4 years (SD: 9.4 years; range: 46-96  
215 years) (Supplementary Table 1). Replication took place in the Core cohort,  
216 consisting of 917 individuals (538 females and 379 males) with a mean age of  
217 33.5 years (SD: 10.7 years; range: 20-60 years) (Supplementary Table 1). The  
218 Manhattan plot identified 14 genome-wide significant ( $P < 5 \times 10^{-8}$ ) independent  
219 loci in discovery GWAS for the first 10 hip shape modes and hip geometric  
220 parameters (Figure 1). Of these, 4 loci were replicated in the Core cohort with  
221 the same direction of effect and a P value < 0.05, including rs35049516  
222 (*SUPT3H*) of HSM4, rs7761119 (*UST*) of HSM8, rs11614913 (*MIR196A2*) of  
223 HSM9, and rs143383 (*GDF5*) of HAL (Table 1). QQ plots showed no inflation  
224 of p values with all genomic inflation factors under 1.04 (Supplementary Figure  
225 1 and Supplementary Table 4). The regional information generated by

226 Locuszoom indicated the strength and extent of the association signal relative  
227 to genomic position (Figure 2, Supplementary Figure 2). Relatively high SNP  
228 heritability was estimated by GCTA in hip morphology GWAS (HSM6:  
229  $h^2 = 0.49$  [95% CI 0.38, 0.59]; HSM3: 0.47 [0.36, 0.57]; HAL: 0.50 [0.40, 0.61];  
230 FNW: 0.46 [0.35, 0.57]; DFH: 0.53 [0.42, 0.64]); HSM5 was estimated to have  
231 a small SNP heritable component (HSM5: 0.17 [0.07, 0.28]) (Supplementary  
232 Table 5). The bivariate GREML analysis showed moderate genetic correlation  
233 between HAL and FN BMD ( $r_G$ : 0.46 [0.27, 0.66]), and also between HSM5  
234 and total hip BMD (0.47 [0.14, 0.79]) (Supplementary Table 6).

235

### 236 **SNP functional annotation**

237 Two of the four SNPs found in the SC cohort to be associated with hip  
238 morphology and successfully replicated in the Core Cohort had a high CADD  
239 score indicating these might be deleterious SNPs (Table 3). Rs11614913, an  
240 exonic SNP in *MIR196A2* (noncoding RNA) associated with HSM9, had a  
241 CADD score of 21.7 and a RegulomeDB score of 5. Moreover, rs143383, a  
242 SNP in UTR5 area of gene *GDF5*, had a CADD score of 21.2. Of those four  
243 replicated SNPs, three SNPs showed significant eQTL associations with  
244 genes in GTEx (Table 3). Rs143383 was found to be an eQTL for several  
245 genes with the strongest evidence being for *UQCC1* ( $P 2.9 \times 10^{-57}$ , tissue  
246 cultured fibroblasts) and *GDF5* ( $P 8.6 \times 10^{-15}$ , tissue esophagus). Rs7761119  
247 was found to be an eQTL for *UST-AS2* ( $P 1.9 \times 10^{-7}$ , tissue cultured fibroblasts)  
248 and *TAB2* ( $P 1.2 \times 10^{-6}$ , tissue cultured fibroblasts). Rs11614913 was also found  
249 to be an eQTL in fibroblasts for *HOXC-AS1* ( $P 2.2 \times 10^{-12}$ ), *GPR84* ( $P 6.6 \times 10^{-5}$ )  
250 and *HOXC8* ( $P 8.3 \times 10^{-5}$ ) (all eQTLs information in supplementary table 2).

251

### 252 **Association with other bone related phenotypes**

253 Associations with OA and other hip-based metrics were evaluated for the four  
254 SNPs found in the SC cohort and successfully replicated in the Core Cohort  
255 (Table 3). Rs35049516 (*SUPT3H*) was found to be protective of OA ( $\beta -0.016$ ,  
256  $P 6.06 \times 10^{-3}$ ) and and HOA ( $\beta -0.058$ ,  $P 1.85 \times 10^{-5}$ ) and positively associated  
257 with HSM4 (a narrower femoral neck and larger femoral head,  $\beta 0.12$ ,  $P$   
258  $4.79 \times 10^{-9}$ ). Rs143383 (*GDF5*) was found to be protective of both OA ( $\beta -0.03$ ,  
259  $P 1.06 \times 10^{-11}$ ) and HOA ( $\beta -0.025$ ,  $P 6.61 \times 10^{-3}$ ) and positively associated with  
260 HAL ( $\beta 0.46$ ,  $P 1.07 \times 10^{-9}$ ). Rs11614913 (*MIR196A2*), which was positively  
261 associated with HSM9 (a wider femoral neck and larger femoral head,  $\beta 0.12$ ,  
262  $P 2.76 \times 10^{-10}$ ) was protective of hip fracture ( $\beta -0.078$ ,  $P 1.30 \times 10^{-7}$ ).

263

### 264 **Overlap with previous largest HSM GWAS study**

265 Nine SNPs previously found to be associated with a HSM in a European  
266 ancestry GWAS showed nominal significance in the SC GWAS ( $P < 0.05$ ) (8)  
267 (Supplementary Table 3). Seven of nine SNPs were replicated in the SC with a  
268  $P$  value  $< 0.05$ . For example, rs2158915 (*SOX9*) was significantly in negative  
269 association with HSM1 in Caucasian cohorts ( $\beta -0.13$ ,  $P 8.47 \times 10^{-27}$ ), which

270 was also associated with HSM2 ( $\beta$  -0.06, P 0.03), HSM3 ( $\beta$  -0.07, P 0.0037)  
271 and HSM4 ( $\beta$  -0.05, P 0.05) in the SC cohort. Rs1243579, positively  
272 associated with HSM1 in the European ancestry GWAS ( $\beta$  0.12, P  $2.85 \times 10^{-14}$ ),  
273 also showed strong association with HSM2 ( $\beta$  0.11, P  $5.06 \times 10^{-7}$ ) and HSM3 ( $\beta$   
274 0.09, P  $3.01 \times 10^{-6}$ ) in the SC cohort.

## 275 Discussion

276 In this study we present the results from a GWAS of 13 measures of hip  
277 morphology (ten orthogonal HSMs and three hip geometric parameters) that  
278 identified 17 conditionally independent SNPs in the SC cohort. Of these, 4 loci  
279 were replicated in an independent replication called the Core cohort  
280 (rs11614913 in *MIR196A2*, rs143383 in *GDF5*, rs35049516 in *SUPT3H* and  
281 rs7761119 at 6q25.1 near *UST* and *TAB2*). This is the first hip morphology  
282 GWAS performed in a Chinese population and replicated in an independent  
283 Chinese cohort. Although in European populations larger GWAS on HSMs, AA  
284 and minimum joint space width were carried out to decipher genetic  
285 architecture of hip shape and provide insights to osteoarthritis pathogenesis,  
286 this study provided genetic characteristics of non-European populations.

287  
288 Recent observational studies found that cam morphology, larger lesser  
289 trochanter size and wider FNW are associated with higher prevalence of HOA  
290 (6, 37, 38, 39). In our study, we found evidence of overlapping associations  
291 between certain genetic loci and hip morphology and HOA (29). Of the 4  
292 replicated loci, rs35049516 (*SUPT3H*) and rs143383 (*GDF5*), which were  
293 associated with HSM4 (a narrower femoral neck and larger femoral head) and  
294 larger HAL respectively, were both protective of OA and HOA. This indicates a  
295 shared genetic basis between hip morphology and HOA in East Asians, as  
296 previously found in European cohorts (8).

297  
298 One of the replicated SNPs, rs11614913 located in the microRNA *MIR196A2*  
299 gene and the *HOXC* gene cluster of developmental transcription factors(40),  
300 was found to be an eQTL for *HOXC-AS1*, *GPR84*, *HOXC8* in cultured  
301 fibroblasts. Rs11614913 (*MIR196A2*) has been reported to be associated with  
302 bone size of lumbar spine area from DXA scans but has not previously been  
303 associated with hip morphology. Stykarsdottir et al. performed a GWAS of  
304 bone size and found rs11614913 (*MIR196A2*) as the strongest signal. They  
305 suspected the variant might affect the efficiency of miR-196-5p target gene  
306 suppression. Then they conducted experimental induction of *MIR196A2*  
307 (C-alleles or T-alleles) into HEK293T cells and assessed the mRNA expression  
308 by RNA-sequencing. The gene enrichment for the entire set of repressed  
309 genes due to experimental induction of *MIR196A2* were reported to find  
310 embryonic skeletal system morphogenesis, supporting the relevance of  
311 *MIR196A2* for bone morphology (26).



312

313 The other locus first reported to be associated with hip morphology was  
314 rs7761119, an intergenic SNP located near *UST* and *TAB2*. This was found to  
315 be an eQTL for both *UST* and *TAB2* in cultured fibroblasts in GTEx. *TAB2*,  
316 TGF-Beta Activated Kinase 1 (MAP3K7) Binding Protein 2, is known to be  
317 involved in the osteoclast differentiation KEGG pathway, consistent with a role  
318 in hip morphology.

319

320 Rs35049516 was an intronic of *SUPT3H*, which was reported to be associated  
321 with body height and heel bone mineral density (41, 42). In a recent GWAS of  
322 minimum joint space width (mJSW) in European populations, *SUPT3H* was  
323 reported to associated with mJSW, an OA-related hip morphology (10). The  
324 overlap of findings indicated Chinese and Western populations appear to have  
325 similar genetic influences on hip morphology.

326

327 Rs143383 (*GDF5*), a functional SNP in the 5'-untranslated region of *GDF5*,  
328 was responsible not only for developmental dysplasia of the hip (DDH) but also  
329 lumbar disc degeneration and osteoarthritis (43) Miyamoto et al firstly reported  
330 that rs143383 showed significant association with hip and knee osteoarthritis  
331 in East Asian populations, suggesting that decreased *GDF5* expression is  
332 involved in the pathogenesis of osteoarthritis (44). Dai et al. showed there was  
333 an association of rs143383 and DDH susceptibility in a Chinese Han  
334 population by a case-control study (45). Although *GDF5* has been known to be  
335 associated with HAL in female of European ancestry (46), this is the first report  
336 of its association with HAL in East Asian populations. Wu et al found evidence  
337 that rs143384 and rs143383 A alleles both have high frequencies in  
338 non-Africans and show strong extended haplotype homozygosity and high  
339 population differentiation in East Asians, indicating that positive selection has  
340 driven the rapid evolution of these two variants of the human *GDF5* gene (47).  
341 Besides, rs143383 (*GDF5*) was an eQTL for not only *GDF5* but *UQCC1*, which  
342 was an OA candidate gene and might be a relevant gene to hip morphology. In  
343 a GWAS study in the Chinese Han population, rs6060373(*UQCC1*) was shown  
344 to play a role in the etiology of DDH(48). In contrast, in a case-control study of  
345 a Turkish population, *UQCC1* rs6060373 polymorphisms were not associated  
346 with DDH(49). In a recent alpha angle (a proxy for cam morphology) meta  
347 GWAS in the European populations, *UQCC1* was found as a candidate gene  
348 for cam morphology(9). Our finding supported the sharing relevance of  
349 *UQCC1* of hip morphology in Chinese and European populations.

350

351 Our study has several strengths. Firstly, we conducted the first hip morphology  
352 GWAS in an East Asian population, broadening the ancestral diversity of  
353 GWAS looking at hip morphology. Secondly, advanced machine-learning  
354 algorithms were applied to hip DXA scans to extract hip shape modes and hip  
355 geometric parameters, which mirror those applied in UK Biobank. This

356 provides opportunities for trans-ancestral hip morphology GWAS in the future.  
357 There are also some limitations to our study. The sample size is limited by the  
358 small number of East Asian studies that contain hip imaging and paired genetic  
359 data, which precluded the use of techniques such as genetic correlation or  
360 well-powered Mendelian randomization (50, 51). That said, we were  
361 sufficiently powered to discover and replicate 4 loci. Further work is needed to  
362 develop large biobanks containing genetic and imaging data in East Asian  
363 populations to allow for comparisons with predominately European ancestral  
364 studies such as UK Biobank and FinnGen (52, 53). The SC cohort is  
365 community-based but not multi-regional, so is not entirely representative of  
366 Chinese populations.

367  
368 In conclusion, our GWAS of hip morphology in Chinese populations identified  
369 four loci, namely rs35049516 (*SUPT3H*) for HSM4, rs7761119 (*UST*) for HSM8,  
370 rs11614913 (*MIR196A2*) for HSM9 and rs143383 (*GDF5*) for HAL. These have  
371 previously been suggested to play an important role in the musculoskeletal  
372 system. However, the present study provides the first evidence that they also  
373 play a similar role in Chinese populations. Further, we identify two novel  
374 independent significant loci, rs11614913 (*MIR196A2*) and rs7761119 (*UST*),  
375 which have not previously been associated with hip morphology. Future  
376 studies with larger sample size and multi-centered Chinese cohorts might be  
377 needed to decipher the genetic factors of hip morphology in the Chinese  
378 population.

## 379 **Acknowledgement**

380 We express our deep appreciation to the members of the Department of  
381 Endocrinology and Metabolism, Zhongshan Hospital for their assistance for  
382 collecting data of the SC cohort. Our study is also supported by the Human  
383 Phenome Data Center of Fudan University. SW is supported by the “Strategic  
384 Priority Research Program” of the Chinese Academy of Sciences (Grant No.  
385 XDB38020400), the CAS Project for Young Scientists in Basic Research  
386 (Grant No. YSBR-077), Shanghai Science and Technology Commission  
387 Excellent Academic Leaders Program (22XD1424700) and Shanghai  
388 Municipal Science and Technology Major Project (Grant No.2017SHZDZX01).  
389 XG is also supported by Shanghai Municipal Science and Technology Major  
390 Project (Grant No. 2017SHZDZX01). BGF is a National Institute of Health and  
391 Care Research Academic Clinical Lecturer and was previously supported by a  
392 Medical Research Council (MRC) clinical research training fellowship (MR/  
393 S021280/1). CL is supported by a Sir Henry Dale Fellowship jointly funded by  
394 the Wellcome Trust and the Royal Society (223267/Z/21/Z). RE was supported  
395 by a Wellcome Trust collaborative award (209233). This research was funded  
396 in whole, or in part, by the Wellcome Trust [Grant numbers: 209233,

397 223267/Z/21/Z]. For the purpose of open access, the author has applied a CC  
398 BY public copyright licence to any Author Accepted Manuscript version arising  
399 from this submission.  
400

## 401 **Author contributions**

402 Conception and study design: JZ, JG, BGF, JHT, XG, SW  
403 Data acquisition: JZ, JG, HL, LJ, XG, SW  
404 Data analysis: JZ, JG  
405 Interpretation of results: JZ, JG, BGF, HL, RE, CL, TC, LJ, JHT, XG, SW  
406 Article drafts were written by JZ, and critically revised by all authors. The final  
407 version of the article was approved by all authors.  
408

## 409 **Declaration of competing interest**

410 No competing financial interests exist.  
411

## 412 **References**

- 413 1. Hunter DJ, Bierma-Zeinstra S. Osteoarthritis. *Lancet*. 2019;393(10182):1745-59.
- 414 2. Zheng J, Frysz M, Faber BG, Lin H, Ebsim R, Ge J, et al. Comparison between UK  
415 Biobank and Shanghai Changfeng suggests distinct hip morphology may contribute to ethnic  
416 differences in the prevalence of hip osteoarthritis. *Osteoarthritis and Cartilage*. 2023.
- 417 3. Lau EM, Lin F, Lam D, Silman A, Croft P. Hip osteoarthritis and dysplasia in Chinese men.  
418 *Ann Rheum Dis*. 1995;54(12):965-9.
- 419 4. Iidaka T, Muraki S, Akune T, Oka H, Kodama R, Tanaka S, et al. Prevalence of  
420 radiographic hip osteoarthritis and its association with hip pain in Japanese men and women:  
421 the ROAD study. *Osteoarthritis Cartilage*. 2016;24(1):117-23.
- 422 5. Park JH, Lee JS, Lee SJ, Kim YH. Low prevalence of radiographic hip osteoarthritis and  
423 its discordance with hip pain: A nationwide study in Korea. *Geriatr Gerontol Int*.  
424 2021;21(1):20-6.
- 425 6. Faber BG, Bredbenner TL, Baird D, Gregory J, Saunders F, Giuraniuc CV, et al.  
426 Subregional statistical shape modelling identifies lesser trochanter size as a possible risk  
427 factor for radiographic hip osteoarthritis, a cross-sectional analysis from the Osteoporotic  
428 Fractures in Men Study. *Osteoarthritis Cartilage*. 2020;28(8):1071-8.
- 429 7. Faber BG, Baird D, Gregson CL, Gregory JS, Barr RJ, Aspden RM, et al. DXA-derived hip  
430 shape is related to osteoarthritis: findings from in the MrOS cohort. *Osteoarthritis Cartilage*.  
431 2017;25(12):2031-8.
- 432 8. Baird DA, Evans DS, Kamanu FK, Gregory JS, Saunders FR, Giuraniuc CV, et al.

- 433 Identification of Novel Loci Associated With Hip Shape: A Meta-Analysis of Genomewide  
434 Association Studies. *J Bone Miner Res.* 2019;34(2):241-51.
- 435 9. Faber BG, Frysz M, Hartley AE, Ebsim R, Boer CG, Saunders FR, et al. A Genome-Wide  
436 Association Study Meta-Analysis of Alpha Angle Suggests Cam-Type Morphology May Be a  
437 Specific Feature of Hip Osteoarthritis in Older Adults. *Arthritis & Rheumatology.*  
438 2023;75(6):900-9.
- 439 10. Faber BG, Frysz M, Boer CG, Evans DS, Ebsim R, Flynn KA, et al. The identification of  
440 distinct protective and susceptibility mechanisms for hip osteoarthritis: findings from a  
441 genome-wide association study meta-analysis of minimum joint space width and Mendelian  
442 randomisation cluster analyses. *eBioMedicine.* 2023;95.
- 443 11. Gao X, Hofman A, Hu Y, Lin H, Zhu C, Jeekel J, et al. The Shanghai Changfeng Study: a  
444 community-based prospective cohort study of chronic diseases among middle-aged and  
445 elderly: objectives and design. *Eur J Epidemiol.* 2010;25(12):885-93.
- 446 12. Frysz M, Faber BG, Ebsim R, Saunders FR, Lindner C, Gregory JS, et al.  
447 Machine-learning derived acetabular dysplasia and cam morphology are features of severe  
448 hip osteoarthritis: findings from UK Biobank. *J Bone Miner Res.* 2022.
- 449 13. Heppenstall SV, Ebsim R, Saunders FR, Lindner C, Gregory JS, Aspden RM, et al. Hip  
450 geometric parameters are associated with radiographic and clinical hip osteoarthritis: findings  
451 from a cross-sectional study in UK Biobank. *medRxiv preprint.* 2023.
- 452 14. Faber B. Geometric Parameters Python 3.0 Code. GitHub 2022 [Available from:  
453 <https://zenodo.org/badge/latestdoi/518486087>].
- 454 15. Zeng H, Ge J, Xu W, Ma H, Chen L, Xia M, et al. Twelve Loci Associated With Bone  
455 Density in Middle-aged and Elderly Chinese: The Shanghai Changfeng Study. *The Journal of*  
456 *Clinical Endocrinology & Metabolism.* 2023;108(2):295-305.
- 457 16. Purcell S, Neale B, Todd-Brown K, Thomas L, Ferreira MAR, Bender D, et al. PLINK: A  
458 Tool Set for Whole-Genome Association and Population-Based Linkage Analyses. *The*  
459 *American Journal of Human Genetics.* 2007;81(3):559-75.
- 460 17. Delaneau O, Coulonges C, Zagury J-F. Shape-IT: new rapid and accurate algorithm for  
461 haplotype inference. *BMC Bioinformatics.* 2008;9(1).
- 462 18. Schork NJ, Howie BN, Donnelly P, Marchini J. A Flexible and Accurate Genotype  
463 Imputation Method for the Next Generation of Genome-Wide Association Studies. *PLoS*  
464 *Genetics.* 2009;5(6).
- 465 19. Heppenstall SV, Ebsim R, Saunders FR, Lindner C, Gregory JS, Aspden RM, et al. Hip  
466 geometric parameters are associated with radiographic and clinical hip osteoarthritis: Findings  
467 from a cross-sectional study in UK Biobank. *Osteoarthritis Cartilage.* 2023.
- 468 20. Jiang L, Zheng Z, Qi T, Kemper KE, Wray NR, Visscher PM, et al. A resource-efficient tool  
469 for mixed model association analysis of large-scale data. *Nature Genetics.*  
470 2019;51(12):1749-55.
- 471 21. D. Turner S. qqman: an R package for visualizing GWAS results using Q-Q and  
472 manhattan plots. *Journal of Open Source Software.* 2018;3(25):731.
- 473 22. Yang J, Lee SH, Goddard ME, Visscher PM. GCTA: A Tool for Genome-wide Complex  
474 Trait Analysis. *The American Journal of Human Genetics.* 2011;88(1):76-82.

- 475 23. Yang J, Ferreira T, Morris AP, Medland SE, Madden PAF, Heath AC, et al. Conditional and  
476 joint multiple-SNP analysis of GWAS summary statistics identifies additional variants  
477 influencing complex traits. *Nature Genetics*. 2012;44(4):369-75.
- 478 24. Pruim RJ, Welch RP, Sanna S, Teslovich TM, Chines PS, Gliedt TP, et al. LocusZoom:  
479 regional visualization of genome-wide association scan results. *Bioinformatics*.  
480 2010;26(18):2336-7.
- 481 25. Lee SH, Yang J, Goddard ME, Visscher PM, Wray NR. Estimation of pleiotropy between  
482 complex diseases using single-nucleotide polymorphism-derived genomic relationships and  
483 restricted maximum likelihood. *Bioinformatics*. 2012;28(19):2540-2.
- 484 26. Styrkarsdottir U, Stefansson OA, Gunnarsdottir K, Thorleifsson G, Lund SH, Stefansdottir  
485 L, et al. GWAS of bone size yields twelve loci that also affect height, BMD, osteoarthritis or  
486 fractures. *Nat Commun*. 2019;10(1):2054.
- 487 27. Zheng HF, Forgetta V, Hsu YH, Estrada K, Rosello-Diez A, Leo PJ, et al. Whole-genome  
488 sequencing identifies EN1 as a determinant of bone density and fracture. *Nature*.  
489 2015;526(7571):112-7.
- 490 28. Nethander M, Coward E, Reimann E, Grahemo L, Gabrielsen ME, Wibom C, et al.  
491 Assessment of the genetic and clinical determinants of hip fracture risk: Genome-wide  
492 association and Mendelian randomization study. *Cell Reports Medicine*. 2022;3(10).
- 493 29. Boer CG, Hatzikotoulas K, Southam L, Stefánsdóttir L, Zhang Y, Coutinho de Almeida R,  
494 et al. Deciphering osteoarthritis genetics across 826,690 individuals from 9 populations. *Cell*.  
495 2021;184(18):4784-818.e17.
- 496 30. Watanabe K, Taskesen E, van Bochoven A, Posthuma D. Functional mapping and  
497 annotation of genetic associations with FUMA. *Nature Communications*. 2017;8(1).
- 498 31. Kircher M, Witten DM, Jain P, O'Roak BJ, Cooper GM, Shendure J. A general framework  
499 for estimating the relative pathogenicity of human genetic variants. *Nat Genet*.  
500 2014;46(3):310-5.
- 501 32. Boyle AP, Hong EL, Hariharan M, Cheng Y, Schaub MA, Kasowski M, et al. Annotation of  
502 functional variation in personal genomes using RegulomeDB. *Genome Research*.  
503 2012;22(9):1790-7.
- 504 33. Ernst J, Kellis M. ChromHMM: automating chromatin-state discovery and characterization.  
505 *Nature Methods*. 2012;9(3):215-6.
- 506 34. Lonsdale J, Thomas J, Salvatore M, Phillips R, Lo E, Shad S, et al. The Genotype-Tissue  
507 Expression (GTEx) project. *Nature Genetics*. 2013;45(6):580-5.
- 508 35. Keen J, Moore H. The Genotype-Tissue Expression (GTEx) Project: Linking Clinical Data  
509 with Molecular Analysis to Advance Personalized Medicine. *Journal of Personalized Medicine*.  
510 2015;5(1):22-9.
- 511 36. Carithers LJ, Moore HM. The Genotype-Tissue Expression (GTEx) Project.  
512 *Biopreservation and Biobanking*. 2015;13(5):307-8.
- 513 37. Baird DA, Paternoster L, Gregory JS, Faber BG, Saunders FR, Giuraniuc CV, et al.  
514 Investigation of the Relationship Between Susceptibility Loci for Hip Osteoarthritis and Dual X-  
515 Ray Absorptiometry-Derived Hip Shape in a Population - Based Cohort of

- 516 Perimenopausal Women. *Arthritis & Rheumatology*. 2018;70(12):1984-93.
- 517 38. Abdulrahim H, Jiao Q, Swain S, Sehat K, Sarmanova A, Muir K, et al. Constitutional  
518 morphological features and risk of hip osteoarthritis: a case-control study using standard  
519 radiographs. *Ann Rheum Dis*. 2021;80(4):494-501.
- 520 39. van Buuren MMA, Arden NK, Bierma-Zeinstra SMA, Bramer WM, Casartelli NC, Felson  
521 DT, et al. Statistical shape modeling of the hip and the association with hip osteoarthritis: a  
522 systematic review. *Osteoarthritis Cartilage*. 2021;29(5):607-18.
- 523 40. Pineault KM, Wellik DM. Hox Genes and Limb Musculoskeletal Development. *Current*  
524 *Osteoporosis Reports*. 2014;12(4):420-7.
- 525 41. Morris JA, Kemp JP, Youten SE, Laurent L, Logan JG, Chai RC, et al. An atlas of genetic  
526 influences on osteoporosis in humans and mice. *Nature Genetics*. 2018;51(2):258-66.
- 527 42. Yengo L, Vedantam S, Marouli E, Sidorenko J, Bartell E, Sakaue S, et al. A saturated map  
528 of common genetic variants associated with human height. *Nature*. 2022;610(7933):704-12.
- 529 43. Gkiatas I, Boptsi A, Tserga D, Gelalis I, Kosmas D, Pakos E. Developmental dysplasia of  
530 the hip: a systematic literature review of the genes related with its occurrence. *EFORT Open*  
531 *Reviews*. 2019;4(10):595-601.
- 532 44. Miyamoto Y, Mabuchi A, Shi D, Kubo T, Takatori Y, Saito S, et al. A functional  
533 polymorphism in the 5' UTR of GDF5 is associated with susceptibility to osteoarthritis. *Nature*  
534 *Genetics*. 2007;39(4):529-33.
- 535 45. Dai J, Shi D, Zhu P, Qin J, Ni H, Xu Y, et al. Association of a single nucleotide  
536 polymorphism in growth differentiate factor 5 with congenital dysplasia of the hip: a  
537 case-control study. *Arthritis Research & Therapy*. 2008;10(5).
- 538 46. Vaes RBA, Rivadeneira F, Kerkhof JM, Hofman A, Pols HAP, Uitterlinden AG, et al.  
539 Genetic variation in the GDF5 region is associated with osteoarthritis, height, hip axis length  
540 and fracture risk: the Rotterdam study. *Annals of the Rheumatic Diseases*.  
541 2008;68(11):1754-60.
- 542 47. Mailund T, Wu D-D, Li G-M, Jin W, Li Y, Zhang Y-P. Positive Selection on the  
543 Osteoarthritis-Risk and Decreased-Height Associated Variants at the GDF5 Gene in East  
544 Asians. *PLoS ONE*. 2012;7(8).
- 545 48. Huang Q, Sun Y, Wang C, Hao Z, Dai J, Chen D, et al. A Common Variant Of  
546 Ubiquinol-Cytochrome c Reductase Complex Is Associated with DDH. *Plos One*. 2015;10(4).
- 547 49. Gumus E, Temiz E, Sarikaya B, Yuksekdog O, Sipahioglu S, Gonel A. The Association  
548 Between BMP-2, UQCC1 and CX3CR1 Polymorphisms and the Risk of Developmental  
549 Dysplasia of the Hip. *Indian Journal of Orthopaedics*. 2020;55(1):169-75.
- 550 50. Bulik-Sullivan B, Finucane HK, Anttila V, Gusev A, Day FR, Loh PR, et al. An atlas of  
551 genetic correlations across human diseases and traits. *Nat Genet*. 2015;47(11):1236-41.
- 552 51. Sanderson E, Glymour MM, Holmes MV, Kang H, Morrison J, Munafò MR, et al.  
553 Mendelian randomization. *Nature Reviews Methods Primers*. 2022;2(1):6.
- 554 52. Littlejohns TJ, Holliday J, Gibson LM, Garratt S, Oesingmann N, Alfaro-Almagro F, et al.  
555 The UK Biobank imaging enhancement of 100,000 participants: rationale, data collection,  
556 management and future directions. *Nature Communications*. 2020;11(1):2624.
- 557 53. Kurki MI, Karjalainen J, Palta P, Sipilä TP, Kristiansson K, Donner K, et al. FinnGen:  
558 Unique genetic insights from combining isolated population and national health register data.  
559 2022.

560

561

Table 1 Independent loci identified in the SC cohort and the replication in the Core cohort

Phenotype	Locus	Lead SNP	Nearest Genes	Discovery				Replication			
				EA/NEA	MAF_SC	Beta	P-value	SNP for replication	EA/NEA	Beta	P-value
HSM1	4q34.1	rs13112214	SCRG1	G/A	0.34	-0.11	2.20E-08	rs13112214	G/A	-0.02	0.59
HSM1	13q14.11	rs498883	KBTBD7	G/A	0.39	-0.10	4.67E-08	rs498883	G/A	-0.06	0.15
HSM2	14q32.2	rs76882404	LINC01550	A/G	0.28	0.13	3.36E-08	rs76882404	A/G	0.03	0.60
HSM3	12q15	rs10878984	FRS2	C/T	0.35	0.11	2.90E-09	rs10878984	C/T	0.07	0.13
HSM4	6p21.1	rs35049516	SUPT3H	TA/A	0.33	0.12	4.28E-09	Proxy SNP: rs12529490	C/A	0.10	<b>0.043</b>
HSM6	17p12	rs2098084	PMP22	A/C	0.41	0.11	1.90E-09	rs2098084	A/C	-0.02	0.56
HSM8	1p21.1	rs12756209	COL11A1	A/C	0.30	0.14	6.76E-11	rs12756209	A/C	0.05	0.40
HSM8	6q25.1	rs7761119	UST, TAB2	T/C	0.27	0.12	1.74E-08	Proxy SNP: rs1934217	G/T	0.10	<b>0.048</b>
HSM8	7p15.1	rs978236	CREB5	C/T	0.26	-0.13	6.98E-09	rs978236	C/T	-0.06	0.18
HSM9	1p12	rs1701987	PSMC1P12, TBX15	G/A	0.22	-0.12	4.92E-08	rs1701987	G/A	-0.01	0.84
HSM9	6p21.1	rs376707397	SUPT3H	T/G	0.27	-0.12	1.11E-08	rs376707397	T/G	-0.09	0.081
HSM9	12p11.22	rs2881860	CCDC91	A/T	0.41	0.11	3.09E-08	rs2881860	A/T	0.03	0.53
HSM9	12q13.13	rs11614913	MIR196A2	C/T	0.44	0.12	2.76E-10	rs11614913	C/T	0.11	<b>0.015</b>
HSM10	12q13.13	rs4759319	HOXC4	T/G	0.43	0.11	4.04E-08	rs4759319	T/G	0.07	0.13
HAL	20q11.22	rs143383	GDF5	G/A	0.28	0.46	9.41E-10	rs143383	G/A	0.44	<b>0.000125</b>
DFH	19p13.3	rs34978235	DOT1L	A/AT	0.40	0.12	3.68E-10	Proxy SNP: rs34978235	G/A	-0.02	0.70
FNW	12p11.22	rs258410	KLHL42, PTHLH	C/A	0.48	-0.20	4.97E-08	rs258410	C/A	-0.07	0.44

Abbreviations: CHR – Chromosome; SNP – single-nucleotide polymorphism; EA - Effect Allele; NEA – Non-Effect Allele; MAF - Minor Allele Frequency; Beta - effect estimate. P-values of replication under 0.05 were marked bold.



Table 2 SNP associations with previous GWAS of OA and hip-based metrics

Shanghai Changfeng cohort					GO Consortium (All OA)		GO Consortium (HOA)		Hip fracture		FN BMD		DXA Bone Area (Total hip area)	
Pheno	Lead SNP	Locus	EA	Beta	Beta	P-value	Beta	P-value	Beta	P-value	Beta	P-value	Beta	P-value
HSM1	rs13112214	4q34.1	G	-0.11	-4.00E-04	0.94	-0.0067	0.52	-0.0097	0.5515	0.0087	0.6339	0.013	0.12
HSM1	rs498883	13q14.11	G	-0.10	-0.0014	0.83	0.0153	0.23	-0.0072	0.7166	-0.0112	0.0556	-0.032	<b>7.21E-03</b>
HSM2	rs76882404	14q32.2	A	0.13	0.01	0.31	0.0366	0.07	-0.0553	0.08258	0.0158	0.7471	-0.028	0.17
HSM3	rs10878984	12q15	C	0.11	-0.017	<b>4.68E-04</b>	-0.0311	<b>9.20E-04</b>	-0.0409	<b>0.007723</b>	-0.0080	0.0684	-0.05	<b>1.87E-09</b>
HSM4	rs35049516	6p21.1	TA	0.12	-0.016	<b>6.06E-03</b>	-0.058	<b>1.85E-05</b>	NA	NA	NA	NA	NA	NA
HSM6	rs2098084	17p12	A	0.11	0.0053	0.52	0.0223	0.18	0.0044	0.8728	0.0152	0.8151	0.028	<b>0.049</b>
HSM8	rs12756209	1p21.1	A	0.14	-0.022	<b>1.19E-04</b>	-0.0666	<b>3.87E-08</b>	0.039	<b>0.03083</b>	-0.0218	0.0568	0.079	<b>4.45E-21</b>
HSM8	rs7761119	6q25.1	T	0.12	0.007	0.13	-0.0053	0.57	-0.0084	0.5803	0.0013	0.8728	-0.017	<b>0.043</b>
HSM8	rs978236	7p15.1	C	-0.13	-0.0036	0.43	-0.0181	<b>0.044</b>	-0.0016	0.9131	0.0112	0.1439	0.00053	0.95
HSM9	rs1701987	1p12	G	-0.12	-0.0037	0.41	0.0046	0.61	-0.0214	0.1468	-0.0080	0.3005	0.00034	0.97
HSM9	rs376707397	6p21.1	T	-0.12	-0.0132	0.14	-0.0089	0.67	-0.0101	0.7194	NA	NA	NA	NA
HSM9	rs2881860	12p11.22	A	0.11	-0.0055	0.31	-0.038	<b>3.20E-04</b>	0.0655	<b>1.609E-04</b>	-0.0236	<b>0.0102</b>	0.029	<b>3.42E-03</b>
HSM9	rs11614913	12q13.13	C	0.12	0.0027	0.55	0.0065	0.48	-0.0782	<b>1.297E-07</b>	NA	NA	-0.0095	0.25
HSM10	rs4759319	12q13.13	T	0.11	-0.0047	0.32	-0.0028	0.76	0.0741	<b>1.358E-06</b>	-0.0409	<b>3.23E-07</b>	0.0075	0.37
HAL	rs143383	20q11.22	G	0.46	-0.032	<b>1.06E-11</b>	-0.0254	<b>6.61E-03</b>	0.0115	0.4459	0.0168	0.073586	0.08	<b>1.71E-20</b>
DFH	rs34978235	19p13.3	A	0.12	-0.0028	0.68	NA	NA	NA	NA	NA	NA	NA	NA
FNW	rs258410	12p11.22	C	-0.20	0.0123	<b>7.67E-03</b>	0.0576	<b>2.73E-10</b>	-0.0378	<b>0.01131</b>	-0.0096	0.2128	-0.024	<b>4.08E-03</b>

Abbreviations : CHR – Chromosome; BP – Position in base pairs; EA – Effect Allele; Beta – Effect estimate; GO – Genetics of Osteoarthritis; HOA – Hip osteoarthritis; FN BMD – Femoral Neck Bone Mineral Density. P-values under 0.05 were marked bold.

Table 3 SNP function of the replicated lead SNPs

Phenotype	Lead SNP	Locus	Func	CADD	RDB	Chromatin state chondrocyte	Chromatin state osteoblast	eQTL
HSM4	rs35049516	6p21.1	intronic	0.552	NA	15	15	NA
HSM8	rs7761119	6q25.1	intergenic	0.091	4	15	15	<i>UST-AS2, TAB2</i> in fibroblasts
HSM9	rs11614913	12q13.13	ncRNA_exonic	21.7	5	14	7	<i>HOXC-AS1, GPR84, HOXC8</i> in fibroblasts
HAL	rs143383	20q11.22	UTR5	21.2	NA	15	15	<i>UQCC1</i> in fibroblasts, <i>GDF5</i> in esophagus

Abbreviations: SNP – single-nucleotide polymorphism; CHR – Chromosome; BP – Position in base pairs.

Func: Functional consequence of the SNP on the gene obtained from ANNOVAR.

CADD: CADD score which is computed based on 63 annotations.

RDB: RegulomeDB score which is the categorical score (from 1a to 7). 1a is the highest score that the SNP has the most biological evidence to be regulatory element.

Chromatin state chondrocyte (from 1 to 15, lower number higher activity).

Chromatin state osteoblast (from 1 to 15, lower number higher activity).

Figure 1: Manhattan plot of the discovery GWAS in the SC cohort

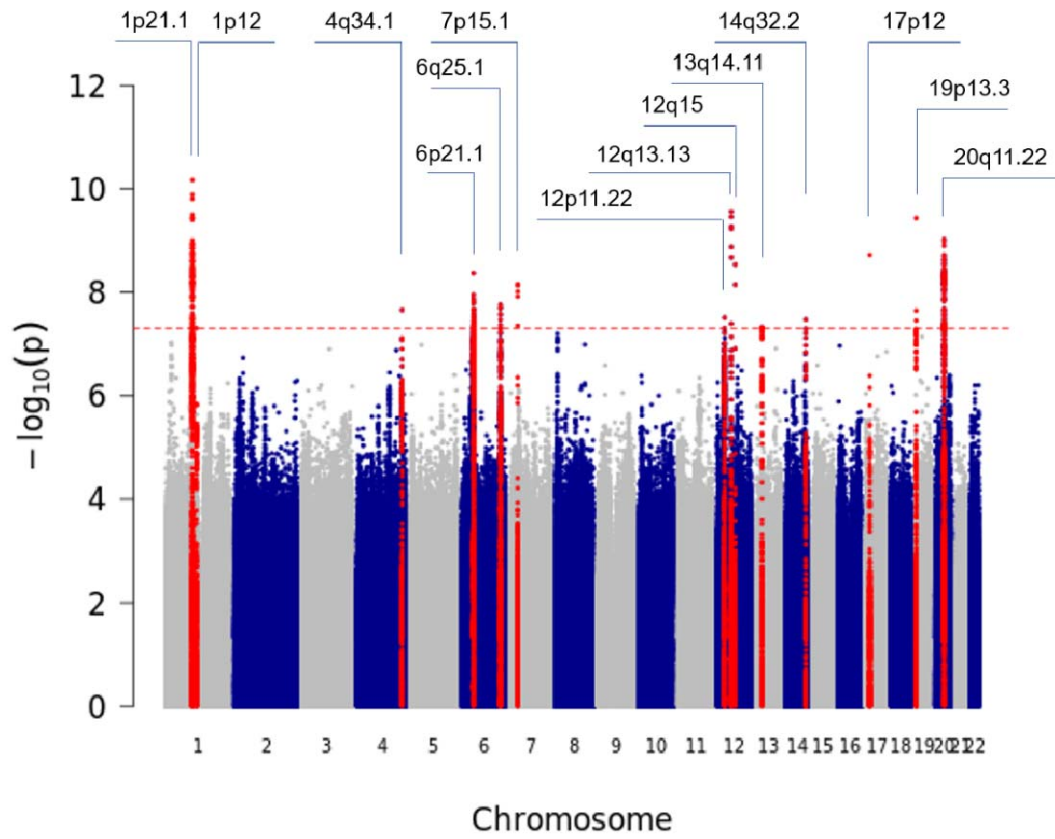


Figure 2: Locuszoom plots of the four replicated loci

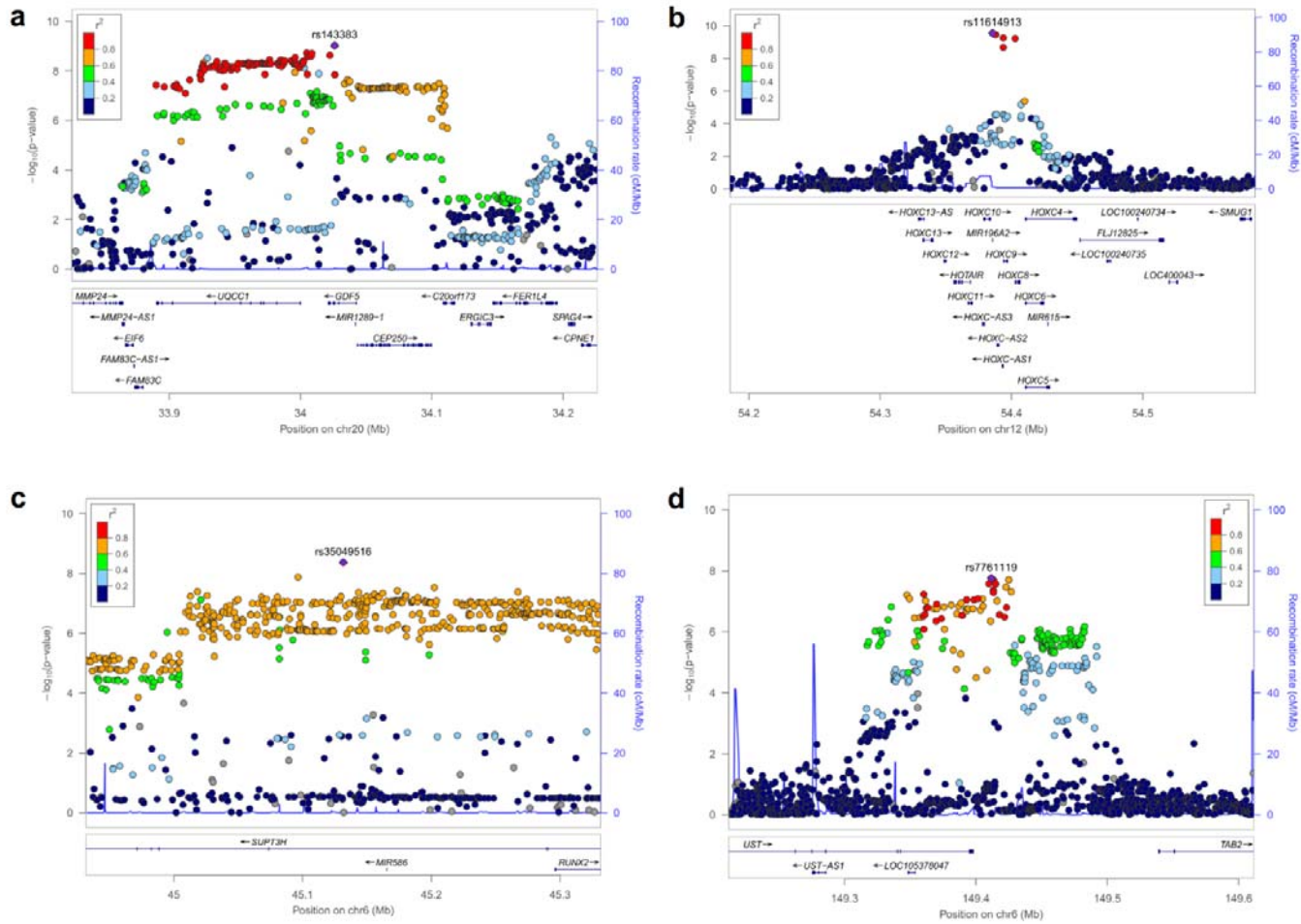
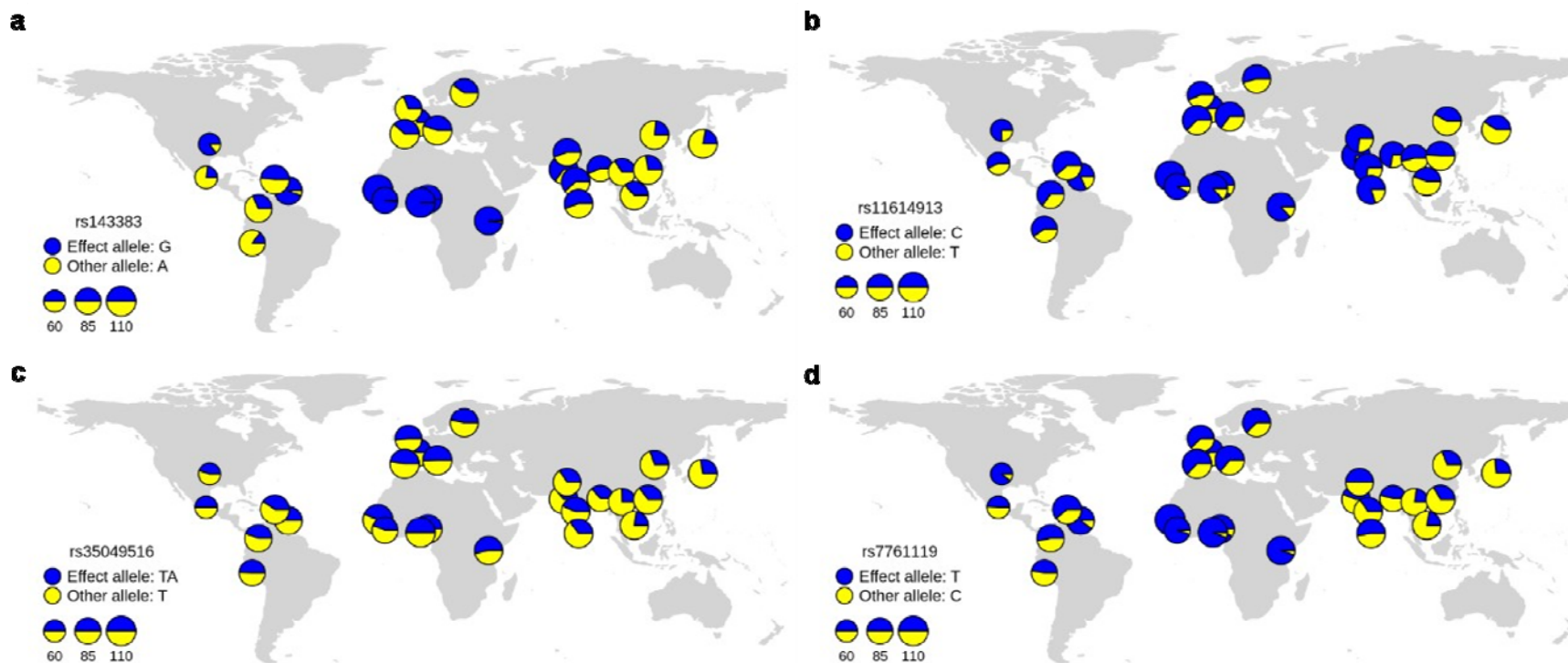


Figure 3: Geographical distribution of associated SNP allele frequencies



Allele frequencies (a) rs143383 (GDF5), (b) rs11614913 (MIR196A2), (c) rs35049516 (SUPT3H) and (d) rs7761119 (UST) were obtained from the 1000 Genome Project and visualized by the R package rworldmap. Effect alleles are marked by blue, and other alleles are marked by yellow. Each pie chart reflects the sample size and frequency of alleles in each subgroup.